MM Science Journal | www.mmscience.eu
ISSN 1803-1269 (Print) | ISSN 1805-0476 (On-line)
Special Issue | HSM 2019
15th International Conference on High Speed Machining
October 8-9, 2019, Prague, Czech Republic
DOI: 10.17973/MMSJ.2019_11_2019064

HSM2019-070

DEVELOPMENT OF A METHOD TO DETERMINE CUTTING FORCES BASED ON PLANNING AND PROCESS DATA AS CONTRIBUTION FOR THE CREATION OF DIGITAL PROCESS TWINS

A. Hänel[1]*, E. Wenkler[1], T. Schnellhardt[1], C. Corinth[2], A. Brosius[1], A. Fay[2], A. Nestler[1]

[1]Technische Universität Dresden, Institute of Manufacturing Technology, Dresden, Germany

[2]Helmut Schmidt University / University of the Federal Armed Forces Hamburg, Institute of Automation Technology, Hamburg, Germany

*Corresponding author; e-mail: albrecht.haenel@tu-dresden.de

Abstract
A digital process twin unifies information from planning and manufacturing of a machining process. Calculation and technological models allow the prediction of further information, which normally is not provided. The work shows the recording of both data sources and creation of a digital process twin for a milling application. Further the usage of technological models is shown at the example of cutting force calculation based on drive currents in combination with a material removal simulation. Also the expansion of digital process twin information for further usage in calculations and visualizations is shown on the example of a part with a high-performance material of the aerospace industry.

Keywords:
Digital process twin; Machine data collection; Cutting forces; Process data; Milling

1 INTRODUCTION

The increasing digitalization of manufacturing opens up numerous possibilities for increasing productivity and effectiveness, especially in the machining of parts [Botkina 2018]. The basic requirement for this is a connection of all information sources involved in the production process as well as automation [Byrne 2016].

A central challenge for research and development is to generate detailed information and knowledge from these data using suitable calculation algorithms, simulation models and intelligent data processing methods [Altintas 2017]. The aim is therefore to generate a digital image or a digital twin from all existing information of an immaterial or material object [Stark 2019]. The same basic challenges also exist in the creation of a digital image of a manufacturing process in the field of machining. The difference is that the focus is limited to a single process only, therefore the term digital process twin (DPT) was chosen.

A digital image of a real machining process or a DPT consists of planning data (target information), process data (actual information) which are recorded during machining. Tool data, machine data and material data are also a part of the DPT.

These data is combined using calculation algorithms and simulation models to represent the machining process for a finished part with as much detail as possible. A further requirement is that the DPT has to be generated as parallel and automated to the machining process as possible. This means that with the start of a milling operation on a machine tool, the DPT is generated and exists at the end of the operation in addition to the real milled part.

The DPT has the requirement to contain geometric and physical information (e.g. the cutting force) from the machining process, for which corresponding methods of determination and calculation must be implemented [Altintas 2014].

The DPT can be used for analysis and documentation purposes, e.g. to compare the nominal path and the actual path of the tool. Another field of application is process visualization, e.g. to detect unnecessary axis movements and in consequence adapt the planning data. [Armendia 2019]

It is also possible to determine more efficient technological setting parameters, such as the feed rate or the cutting depth. However, this represents the highest demand and is significantly dependent on the used calculation algorithms and simulation models. The cutting force represents an important process parameter for the evaluation of a machining process and is therefore an essential component of the DPT [Aslan 2018].

Therefore, the following scientific elaboration presents a method for determining the cutting force on the basis of the planning and process data existing in the DPT. In addition, the basic structure of a DPT and a method for determining relevant data and information from the manufacturing environment is described.

2 AQUISION AND DATA STORAGE

For the DPT creation, which is necessary to completely describe the machining process, the different information sources of the manufacturing process have to be linked. A possible method is described below.

2.1 Gathering information

The information sources for the DPT are located in different areas of the entire manufacturing and development process chain. Basically, these data sources can be classified into planning and process data according to their types of information. For data gathering, it is also relevant whether this information is time-dependent or time-independent.

Gathering information from planning data

The following data or information has to be assigned to the planning data and is required for the creation of a DPT:

- Technology information (CAD/CAM)
- NC-code
- Tool information
- Workpiece information
- Machine information
- Clamping information
- Product information

This information can be considered as time-independent because its content is known before the start of production. It is gathered from the given data sources within the DPT before the start of the machining process.

Gathering information from process data

The control and regulation of modern machine tools is carried out by NC ("numerical control") and PLC ("Programmable Logic Controller"). All measurement and control signals from the sensors and actuators of the machine tool, which represent the process data, converge in the NC and the PLC.

The following control and drive signals are to be recorded as process data for the complete reproduction of the machining task. The following control and drive signals are recorded:

- Actual/ Nominal position data (X, Y, Z, ...)
- Motor drive currents (X, Y, Z, …)
- Spindle current / power
- Spindle speed
- Utilization of drives and spindles
- NC line number
- PLC information: cooling, hydraulics status …

The process data is time-dependent and must be synchronized in the DPT so that the relationship between the individual pieces of information can be analyzed in a time-discrete manner. These process data represent the basic information and can differ depending of the NC system.

2.2 Gathering information as database for the DPT

For process data acquisition, a software tool from the NC systems provider is used, which was installed on a separate measuring and evaluation computer. Communication between the NC / PLC with the measuring and evaluation computer is achieved via a network interface. In order to automate the recording of the process data, an AutoIT software tool called "AutomaticProcessDataAquision" (APDA) was developed. Communication between the NC / PLC and APDA takes place unidirectionally via a shared file folder on the measuring and evaluation computer. The process data acquisition can thus be started via simple block elements in the NC code from the NC, so that the actual recording process can be controlled alongside the machining operation. The process data acquisition is started and stopped for each tool call to the next tool call or the process end. The measurement is then stored separately in the tool related memory of the DPT.

2.3 Creation of the database for the DPT

Figure 1 shows the information model as the basis for the DPT as an UML class diagram.

The *ProcessData* object, modeled as an abstract class, contains all the information of the Process Data document category. The objects *ScopeData* and *CSVData* represent the file types of the various measurement information from the NC.

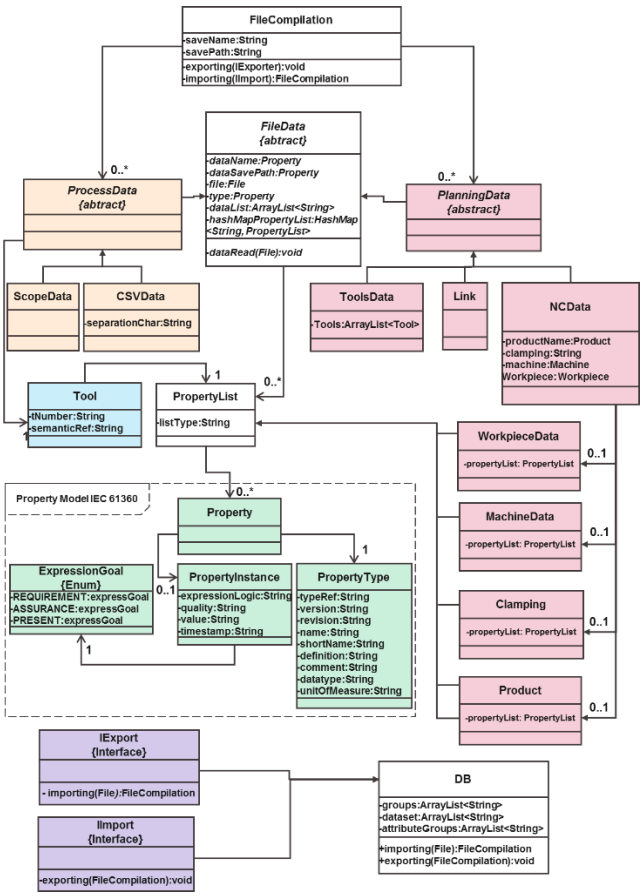

Fig. 1: UML class diagram as basic for DPT.

Each of these objects contain a method that reads the signal information from the corresponding data types and stores it in an array of type string. In addition, further properties of the signal information, if available, is stored as a property in a *PropertyList*. The model of the properties is based on the IEC 61360-1 standardization [IEC 61360]. To describe the characteristics, the ecl@ss characteristics catalogue, which is oriented to IEC 61360, can be used. In the information model, the process data is recorded for each tool of the machining process so that only one tool is assigned to each *ProcessData* element.

The object *PlanningData*, modeled as an abstract class, contains all information of the document type Planning Data. The objects *NCData*, *ToolsData, MachineData, WorkpieceData*, and *Link* are representative for the corresponding file types. As for the process data, the method for data readout of the corresponding file type is also used in the planning data. Depending on the application, either the complete string of the file or only the file pathis saved in the DPT. The *FileCompilation* class combines all information from planning and process data and is later called raw data. This object contains the *importing* and *exporting* methods to convert the processed and merged data into a suitable storage format.

2.4 HDF5 as file format for the DPT

For the storage of the DPT a suitable file format is necessary, which can store and manage large amounts of data as well as assign metadata. A possible storage format is the Hierarchical Data Format (HDF).

HDF is a data file format designed by the National Center for Supercomputing Applications (NCSA) to assist users in the storage and manipulation of scientific data across diverse operating systems and machines. NCSA developed a library of callable routines and a set of utility programs and tools for creating and using HDF files. This work is now performed by The HDF Group [Jenness 2015].

The HDF5 technology suite is designed to organize, store, discover, access, analyse, share, and preserve diverse, complex data in continuously evolving heterogeneous computing and storage environments.

HDF5 supports all types of data stored digitally, regardless of origin or size. Petabytes of remote sensing data collected by satellites, terabytes of computational results from nuclear testing models, and megabytes of high-resolution MRI brain scans are stored in HDF5 files, together with metadata necessary for efficient data sharing, processing, visualization, and archiving [Chen 2016].

With the HDF5 data format the requirements of the DPT for the storage format can be fulfilled.

3 BASIC STRUCTURE OF A DPT

3.1 Calculation models for the DPT

Within section 2 it is shown, that the acquisition and saving of planning and process data is an integral part of the DPT. The raw data itself is usually less informative and can only be interpreted with a good understanding of the process and machine. It is therefore advisable to process the raw data using suitable models in order to increase the information value. This should enable a simple interpretation of the DPT. In order to separate the derived data from the raw data, a distinction must be made between raw data and calculated data, as shown in Figure 2.

The raw data is defined once when the DPT is created. A DPT containing only raw data is also called a digital shadow. The term is intended to clarify that, similar to the shadow of an object, the raw data of a process contains only a subset of all information. As a result, it is difficult to determine the object from the shadow. Equally complex is the connection between measured process data and the process itself.

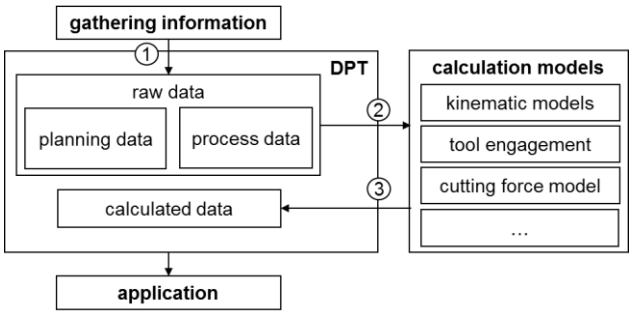

Fig. 2: Data distinction within the DPT.

Therefore, a large number of calculation models are needed to derive more information from the raw data in order to make the DPT usable for analytical purposes.

It is important that the raw data is not changed, similarly to the derivation from the shadow to the shadow throwing object, where the shadow itself remains unchanged. Only the way of interpreting the shadow and the resulting interpretation can be changed, but not the shadow itself.

Transferred to the DPT, this means that the models perform their calculations based on the raw data, but their results are saved separately. This structure allows further models to be integrated, existing models to be adapted and model results to be safely overwritten due to data separation.

3.2 Selected models

General kinematic model

This section is intended to give an overview of possible models showing simple examples. Some standard models are described, which are relevant for each three axis NC machine. It is assumed that the following information can always be recorded from the NC:

- Actual position of each axis s_{act}
- Nominal position of each axis s_{nom}

with:

$$\boldsymbol{s} \in [\boldsymbol{x}, \boldsymbol{y}, \boldsymbol{z}] \tag{1}$$

Since the position changes continuously, the data is available as a list, with one row defining the parameters at a specific point in time.

By directly comparing two adjacent rows, the position change in all axes can be determined, where i is the value of the current line. It is possible to calculate the velocity v, the acceleration a and the jerk j.

$$\overrightarrow{j(t)} = \overrightarrow{\dot{a}(t)} = \overrightarrow{\ddot{v}(t)} = \overrightarrow{\dddot{s}(t)} \tag{2}$$

Normally, a fixed sampling rate t_{sr} is used for data acquisition, which leads to:

$$\Delta t_i = t_{sr} = const. \quad \forall\, i \tag{3}$$

If a constant data rate is not possible, a time stamp has to be recorded.

Equation (2) shows basic kinematic information during the process. Such data is examined, for example, in machine diagnostics. More complex information can also be generated from the data. For example, the feed velocity v_f that can be determined from the axis velocities.

$$v_{f.act} = \sqrt{\sum_{\forall_s} v_{s.act}^2} \tag{4}$$

Normally the programmed feed velocity and the real feed velocity differ due to different control specifics. The nominal feed velocity can also be determined according to equations (2) and (4) by using the nominal values. Afterwards a comprehension is possible.

It can be seen that a wide variety of calculations can be carried out to describe the process with more informative data. With increasing degree of detail, more process-specific information is needed, such as the tool, material, etc.

Further models, such as thermo-energetic calculation models, models for electrical power calculation of the drives or models to determine cutting forces can also be integrated into the DPT. A DPT is therefore not a static representation but can be continuously extended and adapted with calculation models. A detailed example of a more complex model and its evaluation is presented in Section 4.

The model of tool engagement

Various parameters for process evaluation and characterization refer to the tool engagement, e.g.:

- Material removal rate Q_W
- Cutting force F_c
- Tool-life T_L

The tool engagement changes continuously during the process. Therefore, there are no trivial relationships for the de-

termination. bspw. because there is no analytical relationship for the determination of the tool engagement a simulation is required.

The basic idea of an engagement simulation is the determination of the intersection of two bodies (tool and part). The intersection is projected on virtual planes. Then standardized parameters of the tool intervention are derived from the projection. To determine the local engagement, the relative movement is segmented and the engagement is determined for the individual path increment.

Current models distinguish between continuous and discrete approaches. A popular representative of the continuous models is the Constructive-Solid-Geometry model, which achieves the volume as well as the removal by a Boolean combination of simple geometrical volumes (cylinders, cuboids, …) [Weinert 2003]. The continuous approaches are usually very computationally intensive and are therefore used less frequently than discrete approaches.

A discrete representative is the voxel-model, where the workpiece is segmented into small cubes (voxels) with a defined edge length. During tool movement, voxels that are temporarily inside the tool are removed [Jang 2000].

A widespread approach is the dexel-model [Stautner 2006]. In this approach, the volume is projected and segmented along an axis onto a plane. The focal points of the segments are then extruded along the projection axis, creating a parallel line network. Multi-dexel-models combine several dexel models extruded along different axes to increase simulation accuracy.

The calculation effort increases indirectly proportional to the length of the workpiece segmentation, which in turn increases the simulation accuracy.

3.3 DPT extension

Suppose the equations in section 3.2 are to be applied to a new DPT. An example DPT is described below to explain the functionality. The example DPT describes a process with one clamping direction in which a machining program with 5 tools was carried out on a 3-axis machine (see Tab. 1). Since each tool used is logged separately and the tools were only used once, there are 5 logs to be processed.

Tab. 1: Example DPT log information.

Log-No.	Lines	Operation
1	64200	Slab milling
2	15700	Drilling
3	225200	Side milling
4	139600	Side milling
5	22700	Chamfering

In total, the equations must be applied to 467400 entries. Since the equations (2) and (4) and refer to the respective axis, together with equation there are a total of 13 variables to be calculated. This leads to approximately 6.1 million values to be determined. The System to apply the calculation models on a given DPT was implemented in C/C++ and an overview is given in Figure 3.

When the calculation models are called, the DPT is opened and the iteration begins with one clamping direction. For all tool logs in one clamping direction, iteration is performed over the tool logs. For each tool log, the calculation models are applied separately. The log is read and processed line by line. The calculation models determine their values on the basis of the raw data and results are saved in the calculation data.

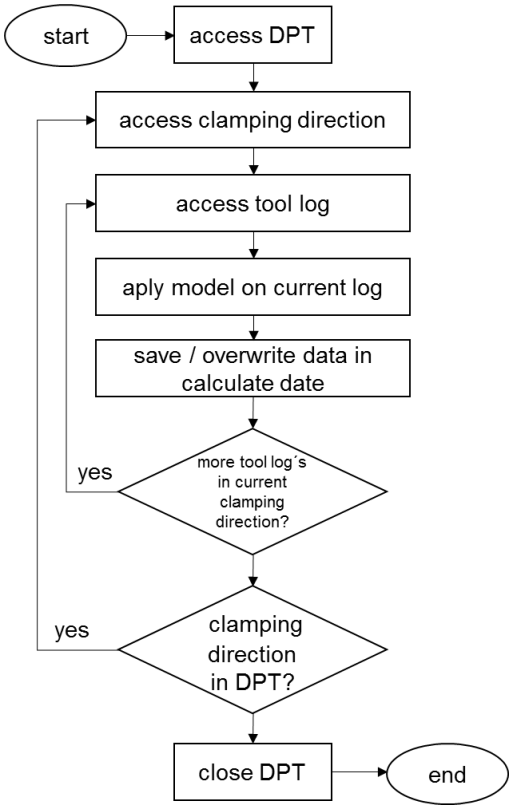

Fig. 3: Flowchart of the calculation models.

The presented prototype logic is only adapted to the requirements of the mentioned models. More complex models may also require cross-log information, which is not supported in this setup and must therefore be integrates separately. For example, in a stock removal simulation, the correct machining sequence must be taken into account, since the state of workpiece changes between machining operations.

4 INTEGRATON OF CUTTING FORCE MODEL IN THE DPT

For optimal planning and design of a milling process, knowledge of the forces occurring during the entire machining process is of great importance. [Adams 2016] Cutting forces are usually measured by external piezoelectric sensors. However, their use is associated with high investment costs, which is why they are usually not used in manufacturing companies. Furthermore, external force sensors impact the handling of the tool and workpiece and are also at risk of destructive overload. For this reason, external piezoelectric force sensors are mostly used for basic investigations in research and not in economic production. Since the motor currents of a machine tool are related to the actual process forces, it is possible to determine the cutting forces indirectly [Arnold 2017, Wenkler 2019].

4.1 Force-modeling based on drive current

The modelling of cutting forces can be carried out both via the current of the feed motors and via the current of the spindle motor [Wenkler 2019]. While statements about the forces in all three physical directions can be made about the feed motor current, the spindle current is limited to model the cutting force. Due to inertia of the mechanical drive components, the bandwidth of the transmission behavior

between force and current is limited for both feed and spindle motors, whereby feed drives generally have a higher bandwidth. The advantage of force modelling based on spindle current is the fact that the spindle is operating at a constant speed during the milling process. In contrast to the feed drive, this reduces the requirement for compensation of the acceleration and static friction components of the drive currents.

In the area of spindle current a model for the calculation of empirical cutting force constants was proposed by Dunwoody [Dunwoody 2010]. Further development of the model was carried out by Aggarwal [Aggarwal 2013].

Because of its simple applicability and good accuracy, this approach has a high practical application potential and is subsequently examined for its applicability as part of the DPT.

4.2 Procedure principle

The method is based on the proportionality between the spindle motor current I and the average power consumed by the spindle P. With the load constant K_I , equation (5) is obtained:

$$I = K_I P \tag{5}$$

Using equation (6) with the angular velocity ω of the spindle and the total torque M applied by the spindle motor, which is composed of a cutting torque M_c and a loss torque M_v according to equation (7) leads to equation (8).

$$P = \omega M \tag{6}$$

$$M = M_c + M_v \tag{7}$$

$$I = K_I \omega (M_c + M_v) \tag{8}$$

With the current loss $I_L(\omega)$ from equation (9) the basic model equation (10) results.

$$I_L(\omega) = K_I \omega M_v \tag{9}$$

$$M_c(I, \omega) = \frac{I - I_L(\omega)}{K_I \omega} \tag{10}$$

To parameterize the model, (9) and (10) must be determined in two steps.

1. The relationship between spindle speed and current loss is determined through air cutting tests ($M_c = 0$).
2. The load meter constant K_I can then be determined by cutting tests with torque, current and speed measurements.

4.3 Parameterization of the model

The model parameterization tests were performed on a WEMAS VZ-1250 Quick 3-axis machining center. The machine is equipped with a Heidenhain TNC620. The spindle motor is a QAN-200UH asynchronous motor. The digital signals of the controller were picked up with a software tool of the controller manufacturer via an Ethernet connection. To determine the current loss $I_L(\omega)$, air cuts were performed in a speed range of $n = 500 \dots 10000\, rpm$ at $n = 500\, rpm$ intervals. The speeds were each held for $10 s$ and the mean torque-forming current was recorded. For each parameter setting three measured values were recorded. The maximum deviation of the measured values was 1.57%.

On the basis of the measured values, the current loss models $I_v(\omega)$ according to Dunwoody (11) and Aggarwal (12) were determined using the method of least squares. The Dunwoody l current loss model is a pure friction model and considers Coulomb friction (K_μ) and viscous friction (K_v). The holistic model according to Aggarwal et al. (12) includes friction parts of the bearing load ($K_{L\mu l}$), spin related friction ($K_{L\mu b}$), viscous friction (K_{Lv}) and windage friction (K_{LRv}) as well as copper losses of the rotor (K_{RCu}) and stator (K_{SCu}) and iron losses (K_{Fe}) and stray losses (with 1.2 % of the cutting power P_c).

$$I_v(\omega) = K_I K_v \omega^2 + K_I K_\mu \omega \tag{11}$$

$$\begin{aligned} I_v(\omega) = {} & K_I K_{2L\mu b} \omega^5 + K_I K_{1L\mu b} \omega^3 \\ & + K_I (K_{LRv} + K_{2Fe}) \omega^2 + K_I K_{Lv} \omega^{\frac{5}{3}} \\ & + K_I \left(K_{0Lvb} + K_{L\mu I} + K_{1Fe}\right) \omega \\ & + K_I (K_{2RCu} + K_{2SCu}) \omega^{-2} \\ & + K_I (K_{0RCu} + K_{0SCu}) \end{aligned} \tag{12}$$

The experimental values and the curves of the two current loss models are shown in Figure 4. It can be seen from the curves that the model of Aggarwal approximates the current loss better than Dunwoody's model and was therefore used for upcoming steps.

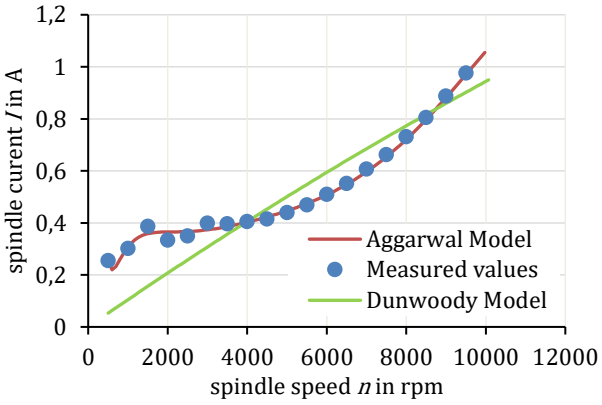

Fig. 4: Results of the air cuts.

Drilling experiments were carried out to determine K_I. A Kistler 4-component dynamometer type 9272 was used to measure the cutting torque. The workpiece material was an alloyed quenched and tempered steel (42CrMo4).

Drills with a diameter of $D = 8\, mm$ and $D = 12{,}5\, mm$ were used to generate different loads on the overall system. The tooth feed was $f_z = 0{,}05 mm$ in each case. The spindle speed was varied in steps of $n = 1000\, rpm$ each from $1000 \dots 10000\, rpm$ for the $D = 8\, mm$ drill. For the $D = 12{,}5\, mm$ drill, the spindle speeds varied from $n = 1000 \dots 6000\, rpm$ were realized.

Figure 5 shows the relationship of the cut current (measured current I minus modeled current loss $I_L(\omega)$) to the measured spindle speed. The course of the measured values can only be described from above spindle speeds between $n = 1500 \dots 2000\, rpm$ by the linear slope of the load meter constant K_I of the model (13).

$$K_I \omega = \frac{I - I_L(\omega)}{M_c} \tag{13}$$

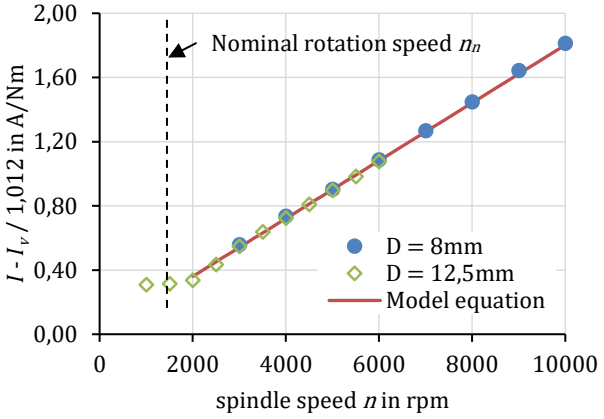

Fig. 5: Results of the drilling tests.

The operating ranges of the spindles asynchronous motor can be used as an explanation for this. In the armature adjustment range of the motor below the nominal rotation speed n_n, the torque can be set only via the torque-forming current, so that a constant ratio between the torque-forming current and the applied torque exists even at a changing speed. For the proportionality factor K_I a value of $2{,}86 * 10^{-5} \frac{A}{W}$ was determined.

4.4 Model validation

In this section, the modeling accuracy of the parameterized model equation is checked. Therefore milling tests were carried out. The forces occurring were determined indirectly via the model using the measured currents and conventionally using a dynamometer (*Kistler type 9272*). On the basis of the measured forces, the coefficients for the empirical cutting nonlinear force model according to Kienzle (14) and a linear cutting force model according to Altintas (15) were calculated.

$$F_c(\varphi) = k_{c1,1} b h_{(\varphi)}{}^{1-m_c} \tag{14}$$

$$F_c(\varphi) = K_{tc} a_p h_{(\varphi)} + K_{te} a_p \tag{15}$$

A stainless martensitic steel (X5CrNiCuNb17-4-4) was used as workpiece material. The tool was a flat end mill with a diameter of $D = 8\,mm$. The speed was set to $n = 5000\,rpm$. A width of cut $a_e = 0{,}5\,mm$ were used. The tooth feed was varied with $f_z = 0{,}2; 0{,}3; 0{,}5; 0{,}8; 1\,mm$. The tests were carried out with depth of cuts equal to $a_p = 2; 4; 6; 8\,mm$. A total of 4 pairs of values ($k_{c1,1}$, m_c, K_{tc}, K_{te}) were determined out of the experiments.

Figures 6 show the cutting force coefficients determined on the basis of the milling tests and their percentage deviation. The progressions of both constants show an increase in the accuracy of the models with increasing of the depth of cut. At a depth of cut with $a_p = 2\,mm$, the deviations are 46,25 % for $k_{c1,1}$ and 208,33 % for m_c.

At a depth of cut with $a_p = 8\,mm$, the deviation drops to 0,66 % or 14.29 % and is therefore within an acceptable range for the Kienzle model. An explanatory approach for the high deviations at low cutting depths is provided by the low forces occurring in combination with low width and depth of cut.

The linear force model according to Altintas shows that at a depth of cut with $a_p = 2\,mm$ the cutting force coefficients in tangential directions K_{tc} deviates only by 6.93%. The edge force coefficient K_{te} also shows also very high deviations at $a_p = 2\,mm$.

Processparameter:
$h_m = 5{,}8 * 10^{-3} \ldots 2{,}9 * 10^{-2}\,mm$ $\quad v_c = 125\,m/min$
$a_e = 0{,}5\,mm$ $\quad f_z = 0{,}2 - 1\,mm$
Workpiece:
X5CrNiCuNb17-4 (1.4548-4)
Toolparameter of the solide cabride flat end mill :
$D = 8\,mm$ $\quad Z = 4$
$\lambda = 35°$ $\quad \gamma = 10°$

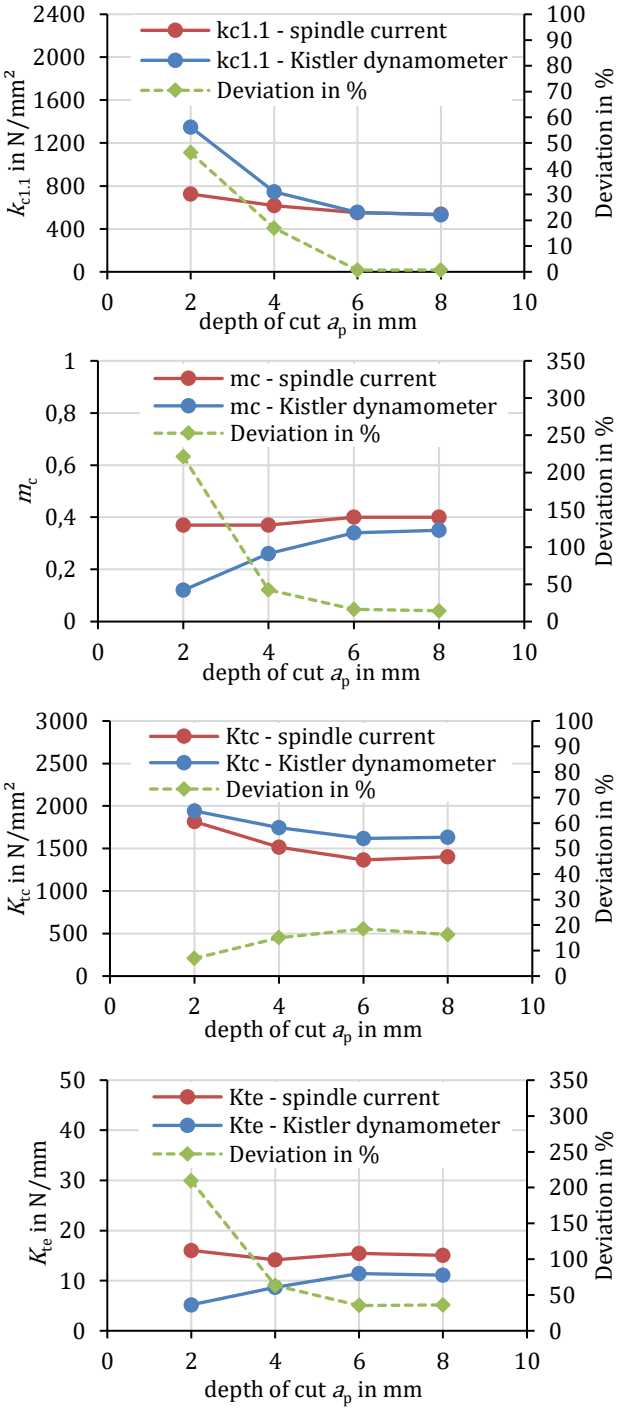

Fig. 6: Cutting force coefficients $k_{c1.1}$, m_c , K_{tc} , K_{te}, and deviation.

In the case of low forces, the torque-forming current components are overlayed by the noise of the drive-current signal and can no longer be clearly identified. As long as the model is used in the speed range above the nominal rotation speed ($n_n = 1500\,rpm$) of the spindle and in the range

of higher forces, it seems to be suitable for the determination of empirical cutting force constants. Due to the combination with the easy handling, the model approach is therefore suitable for use in the DPT.

4.5 Force-model integration to the DPT

To predict cutting forces using the Kienzle model in equation (14) or the Altintas model in equation (15), the engagement parameter are also required in addition to the parameters $k_{c1,1}$, m_c, K_{tc}, K_{te} determined on the basis of the Kienzle or Altintas model. In order to predict a time-discrete force curve, the undeformed chip thickness h and the chip width of undeformed chip b must be given at all times. Since exact quantities for a complex milling process cannot usually be calculated analytically from the process and planning data, a simulation of the material removal must be used, as described in section 3.2. To determine the time-discrete entry angle φ_{in} and exit angle φ_{out} together with the chip width of undeformed chip b of the milling cutter, the material removal simulation must be fed with the following process and planning data from the DPT:

- Actual position of the Tool Center Point (TCP)
- Tool geometry
- Actual workpiece geometry.

For the subsequent calculation of the mean undeformed chip thickness h_m from equation (16), the tooth feed f_z must also be calculated.

$$h_m = \frac{1}{\varphi_c} * \int_{\varphi_{in}}^{\varphi_{out}} h_{(\varphi)} d\varphi = \frac{1}{\varphi_c} * f_z * \sin\kappa \, (\cos\varphi_{in} - \cos\varphi_{out}) \tag{16}$$

$$\overline{F_c} = \frac{Z}{2\pi} \int_{\varphi_{in}}^{\varphi_{out}} F_c d\varphi \tag{17}$$

The tooth feed f_z can also be determined on the basis of the actual position from the TCP. Using the time stamp of the individual tool positions the feed per tooth f_z, can be calculated by numerically differentiating the actual positions in X, Y and Z directions and using the corresponding actual spindle speed.

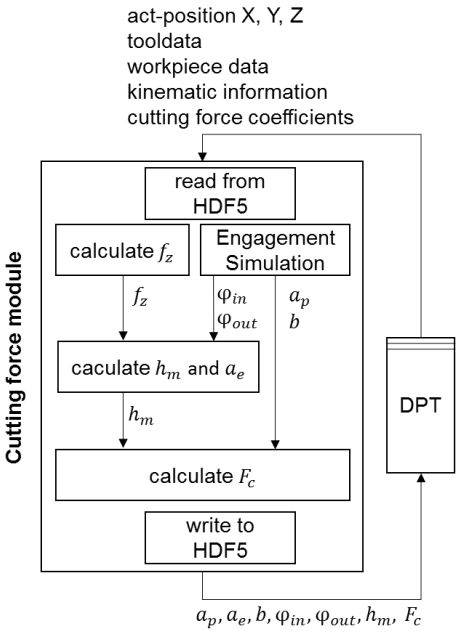

Fig. 7: Cutting force module.

Figure 7 shows the sequence and integration of the cutting force module into the DPT. The module was implemented using C/C++. The ModuleWorks API was used for the material removal simulation, to determine the cutting engagement parameter (Fig. 8). With this module, it is possible to calculate automatically the engagement parameters and the effective cutting forces on the basis of the Kienzle and Altintas models for a complete machining process.

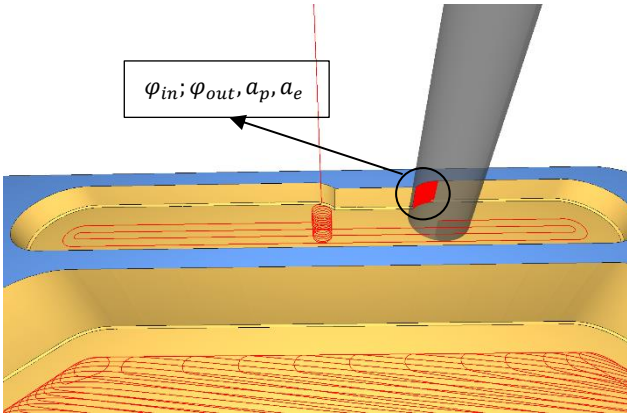

Fig. 8: Material removal simulation with ModuleWorks.

Fig. 8 shows an example of a material removal simulation for milling a slot and its tool path. Fig. 9 shows the curves for the mean cutting forces using the Altintas and Kienzle force models. The mean cutting forces were calculated with equation (17). The cutting force coefficients, which were determined from the spindle current, were used for the calculation (Section 4.4).

Processparameter:

$a_e = 0 \ldots 8\ mm, a_p = 3{,}5\ mm, v_f = 400 \frac{mm}{min}, v_c = 60 \frac{m}{min}$

Workpiece:

X5CrNiCuNb17-4 (1.4548-4)

Toolparameter of the solide carbide flat end mill :

$D = 8\ mm$ $\quad Z = 4$

$\lambda = 35°$ $\quad \gamma = 10°$

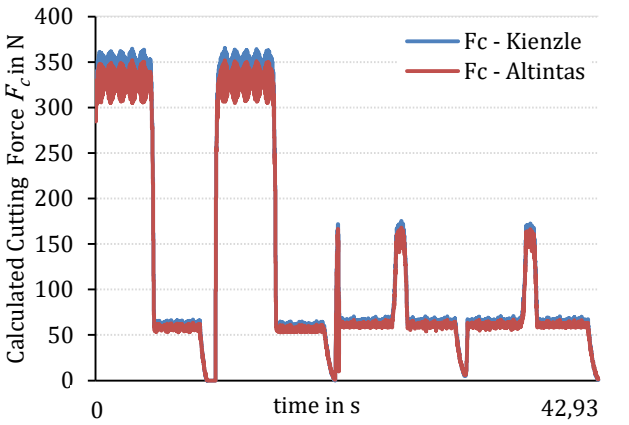

Fig. 9: Cutting force curves for machining the slot.

5 SUMMARY

The first part of this paper describes the basic structure of a DPT for machining and data acquisition. In addition, a selection of possible calculation algorithms and models for the DPT is presented. The second part of the paper describes a method for determining the cutting force and cutting force coefficients according to Kienzle and Altintas on the basis of the spindle current, which is particularly suitable for greater depths and widths of cuts. Finally, a concept for the

implementation of this model in the DPT is described conceptually. This method is only one relevant part of a DPT. In the future, further models are to be integrated in order to present the digital image of the machining process in more detail. The vision is that for each part produced, a DPT exists, in the form of a HDF5 file, which can be used for the analysis and determination of new technological parameters for future machining tasks.

6 ACKNOWLEDGEMENTS

The authors would like to thank the German Federal Ministry for Economic and Technology (BMWi) and VDI/VDE for funding of the research project this study is based on. Bibliography. We would also like to thank ModulWorks, Heidenhain and PMG Precision Mechanics Group GmbH for supporting this research.

7 REFERENCES

[Adams 2016] Adams, O., et al. Model-based Predictive Force Control in Milling – System Identification. Procedia Technology, 2016, Vol. 26, pp. 214-220

[Aggarwal 2013] Aggarwal, S., et al. Cutting Torque and tangential cutting force coefficient identification from spindle motor current. Int. J. Adv Manuf. Technol., 2013, Vol. 65, No, 1-4, pp 81-95

[Altintas 2014] Altintas, P., et al. Virtual process system for part machining operations. CIRP Ann. –Manuf. Technol., 2019, Vol.63, No. 2, pp 585-605

[Altintas 2017] Altintas, P., et al. Integration of virtual and on-line machining process control and monitoring. CIRP Ann. –Manuf. Technol., 2017, Vol.66, No. 1, pp 349-352

[Armendia 2019] Armendia, et. al. Twin-Control - A Digital Twin Approach to Improve Machine Tools Lifecycle. Springer International Publishing, 2019

[Arnold 2017] Arnold, F., et al. New Approaches for the Determination of Specific Values for Process Models in machining Using Artifical Neural Networks. Procedia Manuf., 2017, Vol. 11, No. June, pp 1463-1470

[Aslan 2018] Aslan, D. and Altintas, Y. Prediction of Cutting Forces in Five-Axis Milling Using Feed Drive Current Measurements. IEEE/ASME Trans. Mechatronics, 2018, Vol. 23, No. 2, pp 833-844

[Botkina 2018] Botkina, D., et al. Digital Twin of a Cutting Tool. Procedia CIRP, 2018, Vol. 72, pp 215-218

[Byrne 2016] Byrne, G., et al. High Performance Cutting (HPC) in the New Era of Digital Manufacturing- A Roadmap. Procedia CIRP, 2016, Vol. 46, pp 1-6

[Chen 2016] Chen, Y., et al. The implementation of a data acquisition and services system based on HDF5. Fusion Eng. Des., November 2016, Vol.112, pp 975-978

[Dunwoody 2010] Dunwoody, K. Automated Identification pf cutting Force Coefficients and Tool Dynamics on CNC Machines by.2010, No. March

[IEC 61360] International Electrotechnical Commission. Standard data element types with associated classification scheme – Part 1: Definitions – Principles and methods, 2017

[Jang 2000] Jang, D., et al. Voxel Based Virtual Multi-Axis Machining. Int. J. Adv. Manuf. Technol., August 2000, Vol. 16, No. 10, pp 709-713

[Jenness 2015] Jenness, T. Reimplementing the Hierarchical Data system using HDF5. Astron. Comput, September 2015, Vol. 12, pp 221-228

[Stark 2019] Stark, R., et al. Development and operation of Digital Twins for technical systems and services. CIRP Ann., May 2019

[Stautner 2006] Stautner, M. Simulation und Optimierung der mehrachsigen Fräsbearbeitung. Vulkan Verlag GmbH, 2006

[Weinert 2003] Weinert, K. and Surmann, T. Geometric simulation of the milling process for free formed surfaces. Simul. Aided Offline Process Des. Optim. Manuf. Sculpt. Surfaces, 2003, pp 21-30

[Wenkler 2019] Wenkler, E., et al. Intelligent characteristic value determination for cutting processes based on machine learning. Procedia CIRP, 2019, Vol. 79, No. July, pp 9-14